ASME Paper Title: Sensitivity of Lyapunov Exponents in Design Optimization of Nonlinear Dampers

Authors: Aykut Tamer , Pierangelo Masarati

ASME Journal Title: Journal of Computational Nonlinear Dynamics

Volume/Issue _14/2________________________ Date of Publication (VOR* Online) January 7, 2019_____

ASME Digital Collection URL: https://asmedigitalcollection.asme.org/computationalnonlinear/article/doi/10.1115/1.4 /Sensitivityof-Lyapunov-Exponents-in-Design

DOI: 10.1115/1.4041827

*VOR (version of record)

Sensitivity of Lyapunov Exponents in Design Optimization of Nonlinear Dampers

Aykut Tamer*
Postdoctoral Researcher
Department of Aerospace Science and Technology
Politecnico di Milano
Milano 20156, Italy
Email: aykut.tamer@polimi.it

Pierangelo Masarati
Professor
Department of Aerospace Science and Technology
Politecnico di Milano
Milano 20156, Italy
Email: pierangelo.masarati@polimi.it

This work presents how the analytical sensitivity of Lyapunov Characteristic Exponents can be used in the design of nonlinear dampers, which are frequently utilized to stabilize the response of mechanical systems. The kinetic energy dissipated in the form of heat often induces non-linearities, therefore reducing the reliability of standard stability evaluation methods. Owing to the difficulty of estimating the stability properties of equilibrium solution of the resulting nonlinear time-dependent systems, engineers usually tend to linearize and time-average the governing equations. However, the solutions of nonlinear and time-dependent dynamical systems may exhibit unique properties, which are lost when they are simplified. When a damper is designed based on a simplified model, the cost associated with neglecting nonlinearities can be significantly high, in terms of safety margins that are needed as a safeguard with respect to model uncertainties. Therefore, in those cases, a generalized stability measure, with its parametric sensitivity, can replace usual model simplifications in engineering design, especially when a system is dominated by specific, non-negligible nonlinearities and time-dependencies. The estimation of the characteristic exponents and their sensitivity is illustrated. A practical application of the proposed methodology is presented, considering the problem of helicopter ground resonance and landing gear shimmy vibration with nonlinear dampers are implemented instead of linear ones. Exploiting the analytical sensitivity of the Lyapunov Exponents within a continuation approach, the geometric parameters of the damper are determined. The mass of the damper and the largest characteristic exponent of the system are used as the objective function and the inequality or equality constraint in the design of the viscous dampers.

1 Introduction

Stability is defined as the study of the nearby solutions of an equilibrium under the presence of a perturbation [1]. The stability characteristics of a system strongly depend on the level of nonlinearity and time dependence of the governing equations. If the nonlinear terms can be neglected, a dynamical system either converges, diverges or becomes marginally stable and follows a non-isolated orbit. However, nonlinear systems are more complicated and require deeper understanding for several reasons. First of all, there can exist more than one equilibrium solution, and the trivial solution, i.e. a stationary one, may or may not be one of them [2]. Therefore, stability is not a global property and likely depends on the state of the system. Moreover, there are more complex behaviors in addition to that of linear systems. A typical example is that of limit cycle oscillations (LCO), which are defined as isolated, closed trajectories of non-linear dynamical systems. When an LCO develops, the system os-

*Corresponding Author.

cillates in a self-sustained manner without the need of an external input [3]. The amplitude of an LCO depends on the structure of the system, regardless of the initial conditions, as opposed to non-isolated orbits of marginally stable linear systems. Chaos is another strange behavior, defined as an unpredictable, unstable but bounded motion [2]. Indeed, unlike linear systems, there is no correlation between boundedness and stability of a solution [4]. These phenomena, whose occurrence may have significant effects on the performance of the design, can be detected only if the nonlinearities of the system are not neglected [5, 6].

Stability qualities of a dynamical system can be assessed using different approaches. Examples are experimenting with a physical system or running a simulation in a virtual environment. In both cases, the system is perturbed using an input channel and measuring the decaying characteristics of an output channel. However, stability assessment through experiments and simulation is somewhat limited, since not all the input and output channels can be practically tested or simulated. However, a complete and quantitative understanding of the stability characteristics is possible using spectral methods. The practical, quantitative way of measuring spectra depends on whether a system is autonomous — i.e. non time-dependent — and linear. Linear Time Invariant (LTI) and Linear Time Periodic (LTP) problems typically result from the linearization of nonlinear, non-autonomous problems about a steady (both LTI and LTP) or a periodic (LTP only) reference solution. They rely on eigenanalysis of special matrices and require the existence of such solutions, and the capability to identify and compute them. Obtaining a steady or periodic solution by numerical integration in time requires that solution to be stable; its computation must start from within its region of attraction.

A method that does not require a special reference solution (i.e. a stable point or a stable orbit) but, on the contrary, provides indications about the existence of an *attractor*, being it a point, a periodic orbit or a higher-order solution (e.g. a multidimensional torus), while computing the evolution of the system towards it, would give valuable insight into the system properties and, at the same time, provide a viable and practical means for its analysis. Lyapunov Characteristic Exponents (LCE), or Lyapunov Exponents in short, are indicators of the nature and of the stability properties of solutions of differential equations (see for example [4, 7] and references therein). They define the spectrum of the related Cauchy (initial value) problem. Lyapunov's theory can be applied to nonlinear, time-dependent systems of differential equations. The stability of trajectories in state space can be estimated while computing their evolution. The possibility to extend the approach to systems of differential-algebraic equations, as outlined for example in [8–10], represents a promising development, in view of their use in the formulation of modern multibody dynamics.

In a dynamical system, especially when it is used for design , the rate of change of stability indicators estimates with respect to a parameter plays a significant role when the value of the parameter is expected to change or is uncertain, needs to be modified in later design phases, or is determined by means of an optimization process. Therefore, such sensitivity is useful to gain insight into the dependence of stability indicators on system parameters, or can be integrated into gradient-based (or gradient-aware) optimization procedures [11] and continuation algorithms [12], or into uncertainty evaluation problems. Methods to estimate the sensitivity of stability measures are required, either analytic or numerical. The latter require the calculation of stability measures with and without perturbations in the parameter, followed by finite differences. However, for nonlinear systems, a change in the value of a parameter does not change only the stability properties, but also the reference trajectory, whereas that trajectory does not depend on the perturbation for linear systems. Hence, the development of analytical sensitivity estimation is preferable, to avoid problems related to sharp changes in sensitivity to parameters, and to gain the capability to detect such topology changes of the solution and track them using continuation algorithms.

The estimation of analytical sensitivity of stability indicators has been studied in the literature based on linearity and periodicity assumption (for example, Adrianova in Ref. [4] studied the sensitivity of the spectrum of linear systems to parameter uncertainty; Shih et al. in Ref. [13] discussed parametric sensitivity of nonlinear and periodic systems). An original contribution, introduced by the authors, utilizes the analytical sensitivity of LCE estimates to changes in system parameters for nonlinear, non-autonomous problems [14]. The analytical sensitivity problem is based on the Discrete QR method, which exploits the QR decomposition of the state transition matrix $\mathbf{Y}(t, t_0)$ of a differential problem using the tangent manifold of the so-called fiducial trajectory.

In a design problem, several parameters and components that might affect stability may require close attention. Among them, dampers are specifically aimed at improving the convergent characteristics of the system response, therefore being a rather critical subsystem with respect to stability. The energy dissipation characteristic of dampers often depends on friction, which is intrinsically non-linear and time-dependent. Therefore, even though the rest of the system can be analyzed for stability using a linearized model with acceptable error margins, the addition of dampers can turn an otherwise linear time invariant system into a nonlinear time-dependent one. Therefore, the optimal design of dampers can benefit from the sensitivity of stability indicators obtained without undue linearity assumptions. This work demonstrates the use of the LCE sensitivity estimation, based on the approach formulated in Ref. [14], in design optimization of nonlinear problems, with specific reference to dampers. Section 2 introduces LCEs, their estimation, and that of their sensitivity. Section 3 describes an example problem and an optimization strategy that exploits sensitivity of LCEs. Section 4 presents the validation and optimization results achieved using the proposed method. Finally, some conclusions are drawn.

2 Spectrum of Non-Autonomous Problems and Its Sensitivity

This section briefly recalls the definition of non-autonomous problems and of LCEs as a measure of their spectrum, along with numerical procedures for their estimation, and the procedure for the estimation of their sensitivity to system parameters. Readers may refer to [14] and [15] for more details.

2.1 Non-Autonomous Problems

In engineering practice, initial value, or Cauchy, differential problems of the form

$$\dot{\mathbf{x}} = \mathbf{f}(\mathbf{x}, t), \qquad \mathbf{x}(t_0) = \mathbf{x}_0 \tag{1}$$

often arise. Special cases occur when the problem is linear, i.e. $\mathbf{f}(\mathbf{x},t) = \mathbf{A}(t)\mathbf{x}(t)$, and in particular periodic, i.e. linear with $\mathbf{A}(t+T) = \mathbf{A}(t)$ for a given constant T, called the period, $\forall t$. Autonomous problems arise when $\mathbf{f}(\mathbf{x})$ does not explicitly depend on time t; a special case occurs when the problem is linear, i.e. $\mathbf{f}(\mathbf{x}) = \mathbf{A}\mathbf{x}$, with $\mathbf{A}$ constant, leading to a LTI problem. Stability indicators are the real part of the eigenvalues of matrix $\mathbf{A}$ for LTI systems, the logarithm of the real part of the eigenvalues of the monodromy matrix divided by the period for LTP problems and, as discussed in this work, LCEs for nonlinear, non-autonomous problems, a definition that includes LTI and LTP ones as special cases.

2.2 Lyapunov Characteristic Exponents

Given the problem of Eq. (1), with the state $\mathbf{x} \in \mathbb{R}^n$, the time $t \in \mathbb{R}$, and the nonlinear function $\mathbf{f} \in \mathbb{R}^{n+1} \rightarrow \mathbb{R}^n$, and a solution $\mathbf{x}(t)$ for given initial conditions $\mathbf{x}(t_0) = \mathbf{x}_0$, its Lyapunov Characteristic Exponents λ_i are defined as:

$$\lambda_i = \lim_{t\to\infty} \frac{1}{t} \log \| {}_i\mathbf{x}(t) \| , \tag{2}$$

where ${}_i\mathbf{x}(t)$ is the solution that describes the exponential evolution of the i-th axis of the ellipsoid that grows from an initially infinitesimal n-sphere according to the map $\mathbf{f}_{/\mathbf{x}}$ tangent to $\mathbf{f}$ along the fiducial trajectory $\mathbf{x}(t)$, i.e. the solution of the linear, non-autonomous problem ${}_i\dot{\mathbf{x}}(t) = \mathbf{f}_{/\mathbf{x}}(\mathbf{x}(t),t)\,{}_i\mathbf{x}(t)$, with ${}_i\mathbf{x}(t_0) = {}_i\mathbf{x}_0$. The definition involves the limit for $t \rightarrow \infty$; hence, in practice LCEs can only be numerically estimated for a sufficiently large value of t. In this study, unless explicitly stated, with the term "LCEs" we refer to their estimation using a large enough value of t.

LCEs represent a measure of the rate of growth of perturbed solutions. Consider infinitesimal, independent perturbations of the states with respect to a solution $\mathbf{x}(t)$ of Eq. (2), the fiducial trajectory. Formally, the perturbed solution can be written in terms of the state transition matrix $\mathbf{Y}(t,t_0)$, since it is linear, considering $\mathbf{A}(\mathbf{x},t) = \mathbf{f}_{/\mathbf{x}}$, as the solution of the problem

$$\dot{\mathbf{Y}}(t,t_0) = \mathbf{A}(\mathbf{x},t)\mathbf{Y}(t,t_0), \qquad \mathbf{Y}(t_0,t_0) = \mathbf{I}. \tag{3}$$

2.3 The Discrete QR Method

The definition of Eq. (2) is not practical, because the determinant of the state transition matrix usually either contracts to zero or expands to infinity, depending on the (lack of) stability of the solution, thus either under- or overflowing. Numerical methods have been devised for this purpose. A quite popular one is the so-called Discrete QR method, which is based on incrementally updating the LCE estimates with the contribution of the diagonal elements of the matrix $\mathbf{R}$ resulting from the QR decomposition of the state transition matrix between two consecutive time steps.

Given the state transition matrix $\mathbf{Y}(t,t_{j-1})$ from time t_{j-1} to an arbitrary time t as the solution of the problem $\dot{\mathbf{Y}} = \mathbf{f}_{/\mathbf{x}}(\mathbf{x}(t),t)\mathbf{Y}$ with $\mathbf{Y}(t_{j-1},t_{j-1}) = \mathbf{I}$, set $\mathbf{Y}_j = \mathbf{Y}(t_j,t_{j-1})$. Consider the QR decomposition of $\mathbf{Y}_j\mathbf{Q}_{j-1}$, which implies $\mathbf{Q}_j\mathbf{R}_j = \mathbf{Y}_j\mathbf{Q}_{j-1}$. After defining $\mathbf{R}_{\Pi_j} = \Pi_{k=0}^{j}\mathbf{R}_{j-k}$, one can show that

$$\mathbf{Y}_j\mathbf{Q}_{j-1}\mathbf{R}_{\Pi_{j-1}} = \mathbf{Q}_j\mathbf{R}_j\mathbf{R}_{\Pi_{j-1}} = \mathbf{Q}_j\mathbf{R}_{\Pi_j} = \mathbf{Y}(t_j,t_0) \tag{4}$$

This way, $\mathbf{Q}_j^T\mathbf{Y}_j\mathbf{Q}_{j-1}\mathbf{R}_{\Pi_{j-1}}$ can be used to construct $\mathbf{R}_{\Pi_j}$ by only considering incremental QR decompositions over $\mathbf{Y}_j\mathbf{Q}_{j-1}$, i.e. with limited contraction/expansion.

The LCEs are then estimated from $\mathbf{R}_{\Pi_j}$ as:

$$\lambda_i = \lim_{j\to\infty} \frac{1}{t_j} \log r_{ii}(t_j) = \lim_{j\to\infty} \frac{1}{t_j} \sum_{k=0}^{j} \log(r_{k_{ii}}), \tag{5}$$

where $r_{ii}(t_j)$ are the diagonal elements of matrix $\mathbf{R}(t_j) = \mathbf{R}_{\Pi_j}$.

To calculate LCEs using the QR method, the state transition matrix $\mathbf{Y}(t,t_j)$ is necessary. Usually, analytical integration is not possible; therefore, a numerical approach is needed, which can be obtained by considering a time step small enough to make the assumption of constant Jacobian matrix of the problem, $\hat{\mathbf{A}}$, acceptable. In this case, the state transition matrix can be written as

$$\mathbf{Y}(t,t_j) \approx \mathrm{e}^{\hat{\mathbf{A}}(t-t_j)}\mathbf{Y}(t_j,0), \tag{6}$$

where $\mathbf{Y}(t_j,0)$ results from integration starting from $t=0$, with $\mathbf{Y}(0)=\mathbf{I}$, thus it is available at the current time step t_j. The matrix exponential can be calculated using matrix power series,

$$\mathrm{e}^{\mathbf{A}t} = \mathbf{I} + \mathbf{A}t + \frac{1}{2}\mathbf{A}^2t^2 + \frac{1}{6}\mathbf{A}^3t^3 + \ldots = \sum_{k=0}^{+\infty}\frac{1}{k!}\mathbf{A}^kt^k \tag{7}$$

which can be approximated by truncation at some order of k, depending on the size of the time step.

It is worth stressing that estimating LCEs can be a rather computationally expensive and time consuming process, whose cost is by far not commensurable with computing the eigenvalues of the system matrix, as for LTI problems, nor with computing the monodromy matrix and extracting its eigenvalues, as for LTP ones.

2.4 Sensitivity of Lyapunov Exponents Estimates

Consider a set of bounded parameters $\mathbf{p} \in \mathcal{P}$, and assume that the problem $\dot{\mathbf{x}} = \mathbf{f}(\mathbf{x},t,\mathbf{p})$ depends on the parameters in $\mathbf{p}$. The sensitivity of the LCEs with respect to a generic parameter $p \subset \mathbf{p}$, using the summation form of Eq. 5, can be expressed as

$$\lambda_{i/p} = \lim_{j\to\infty}\frac{1}{t_j}\sum_{k=1}^{j}\frac{r_{k_{ii}/p}}{r_{k_{ii}}}. \tag{8}$$

In this case, only the sensitivity of each of the $\mathbf{R}_j$ matrices is needed, which is obtained in the next section by computing the sensitivity of the QR decomposition.

2.5 Sensitivity of QR Decomposition

The sensitivity of the QR decomposition can be obtained along the lines of the state transition matrix QR decomposition differentiation that is used to formulate the continuous QR method for LCE estimation (see for example [7, 16]).

Consider the QR decomposition of an arbitrary matrix $\mathbf{M} \in \mathbb{R}^{n\times n}$:

$$\mathbf{M} = \mathbf{QR} \tag{9}$$

with $\mathbf{Q}^T\mathbf{Q} = \mathbf{I}$, and $\mathbf{R}$ upper triangular, with positive diagonal elements. Consider the derivative of $\mathbf{M}$ with respect to a scalar parameter p,

$$\mathbf{M}_{/p} = \mathbf{Q}_{/p}\mathbf{R} + \mathbf{Q}\mathbf{R}_{/p}, \tag{10}$$

and the corresponding derivative of the orthogonality condition $\mathbf{Q}^T\mathbf{Q} = \mathbf{I}$,

$$\left(\mathbf{Q}^T\right)_{/p}\mathbf{Q} + \mathbf{Q}^T\mathbf{Q}_{/p} = \mathbf{0}, \tag{11}$$

i.e.

$$\left(\mathbf{Q}^T\mathbf{Q}_{/p}\right)^T + \mathbf{Q}^T\mathbf{Q}_{/p} = \mathbf{0}. \tag{12}$$

The latter condition states that $\mathbf{Q}^T\mathbf{Q}_{/p}$ must be skew-symmetric; thus, only $n(n-1)/2$ coefficients are independent (for example, those in the strictly lower triangular portion, i.e. the lower triangular part, excluding the diagonal).

Finally, premultiply $\mathbf{M}_{/p}$ by $\mathbf{Q}^T$:

$$\mathbf{R}_{/p} = \mathbf{Q}^T\mathbf{M}_{/p} - \mathbf{Q}^T\mathbf{Q}_{/p}\mathbf{R} \tag{13}$$

Since matrix $\mathbf{R}_{/p}$ is upper triangular, the whole problem can be re-cast in the form[1] :

$$\begin{aligned}
\text{compute} \quad & \mathbf{W} = \mathbf{Q}^T\mathbf{Q}_{/p} && \text{(14a)}\\
\text{such that} \quad & \mathrm{stril}\left(\mathbf{Q}^T\mathbf{M}_{/p} - \mathbf{WR}\right) = \mathrm{stril}\left(\mathbf{0}\right) && \text{(14b)}\\
\text{subjected to} \quad & \mathbf{W}^T + \mathbf{W} = \mathbf{0} && \text{(14c)}
\end{aligned}$$

$$\begin{aligned}
\text{compute} \quad & \mathbf{R}_{/p} && \text{(14d)}\\
\text{such that} \quad & \mathrm{triu}\left(\mathbf{R}_{/p}\right) = \mathrm{triu}\left(\mathbf{Q}^T\mathbf{M}_{/p} - \mathbf{WR}\right) && \text{(14e)}\\
\text{and} \quad & \mathrm{stril}\left(\mathbf{R}_{/p}\right) = \mathrm{stril}\left(\mathbf{0}\right). && \text{(14f)}
\end{aligned}$$

The last statement is redundant since $\mathbf{W}$ computed according to Eqs. (14a–c) already yields $\mathbf{R}_{/p}$ with the strictly lower triangular part set to zero.

It is worth noticing that, since $\mathbf{R}$ is upper triangular, $\mathbf{W}$ is computed as

$$\mathbf{W}_L = \mathrm{stril}\left(\mathbf{Q}^T\mathbf{M}_{/p}\mathbf{R}^{-1}\right) \qquad \mathbf{W} = \mathbf{W}_L - \mathbf{W}_L^T \tag{15}$$

[1] Operator $\mathrm{triu}(\cdot)$ extracts the upper triangular part of the argument; operator $\mathrm{stril}(\cdot)$ extracts the strictly lower triangular part of the argument.

where $\mathbf{R}^{-1}$ does not require any factorization, but only back-substitution. In fact, after setting $\mathbf{B} = \mathbf{Q}^T \mathbf{M}_{/p}$, the generic coefficient of stril($\mathbf{W}$) is

$$w_{ij} = \frac{1}{r_{jj}} \left(b_{ij} - \sum_{k=1}^{j-1} w_{ik} r_{kj} \right) \quad j = 1, n-1 \quad i = j+1, n. \tag{16}$$

Then

$$\mathbf{Q}_{/p} = \mathbf{Q}\mathbf{W}. \tag{17}$$

2.6 Sensitivity of Lyapunov Exponents Estimated by the Discrete QR Method

The discrete QR method requires the decomposition of $\mathbf{Y}_j \mathbf{Q}_{j-1}$; thus, the sensitivity of $\mathbf{Y}_j \mathbf{Q}_{j-1} = \mathbf{Q}_j \mathbf{R}_j$ is actually required, i.e.

$$\mathbf{Q}_{j/p}\mathbf{R}_j + \mathbf{Q}_j \mathbf{R}_{j/p} = \mathbf{Y}_{j/p}\mathbf{Q}_{j-1} + \mathbf{Y}_j \mathbf{Q}_{(j-1)/p}, \tag{18}$$

where $\mathbf{Q}_{j-1}$ and $\mathbf{Q}_{(j-1)/p}$ are available from the previous step.

First of all, Eq. (18) is premultiplied by $\mathbf{Q}_j^T$ to obtain

$$\mathbf{Q}_j^T \mathbf{Q}_{j/p}\mathbf{R}_j + \mathbf{R}_{j/p} = \mathbf{Q}_j^T \mathbf{Y}_{j/p}\mathbf{Q}_{j-1} + \mathbf{Q}_j^T \mathbf{Y}_j \mathbf{Q}_{(j-1)/p}. \tag{19}$$

Then the strictly lower triangular part of the equation is evaluated to compute $\mathbf{W}_L$,

$$\begin{aligned} \mathbf{W}_L &= \text{stril}\left(\left(\mathbf{Q}_j^T \mathbf{Y}_{j/p}\mathbf{Q}_{j-1} + \mathbf{Q}_j^T \mathbf{Y}_j \mathbf{Q}_{(j-1)/p} \right) \mathbf{R}_j^{-1} \right) \\ &= \text{stril}\left(\left(\mathbf{Q}_j^T \mathbf{Y}_{j/p}\mathbf{Q}_{j-1} + \mathbf{R}_j \mathbf{W}_{j-1} \right) \mathbf{R}_j^{-1} \right), \end{aligned} \tag{20}$$

the strictly lower triangular part of $\mathbf{W}_j = \mathbf{Q}_j^T \mathbf{Q}_{j/p} = \mathbf{W}_L - \mathbf{W}_L^T$. See Eq. (16) for details about the computation of $\mathbf{W}_L$.

Finally, the upper triangular part of Eq. (19) is evaluated to obtain $\mathbf{R}_{j/p}$,

$$\begin{aligned} \mathbf{R}_{j/p} &= \mathbf{Q}_j^T \left(\mathbf{Y}_{j/p}\mathbf{Q}_{j-1} + \mathbf{Y}_j \mathbf{Q}_{(j-1)/p} \right) - \mathbf{W}_j \mathbf{R}_j \\ &= \mathbf{Q}_j^T \mathbf{Y}_{j/p}\mathbf{Q}_{j-1} + \mathbf{R}_j \mathbf{W}_{j-1} - \mathbf{W}_j \mathbf{R}_j \end{aligned} \tag{21}$$

The sensitivity of $\mathbf{Y}_j$, i.e. the state transition matrix from t_{j-1} to t_j, is needed.

2.7 Sensitivity of the State Transition Matrix

The sensitivity of $\mathbf{Y}$ at time t_j, namely $\mathbf{Y}_{/p}(t_j)$, is needed to compute the sensitivity of the LCEs. In principle, this is obtained by integrating the sensitivity of the problem $\dot{\mathbf{Y}} = \mathbf{A}\mathbf{Y}$. Then

$$\begin{aligned} \dot{\mathbf{Y}}_{/p} &= \mathbf{A}\mathbf{Y}_{/p} + \left(\mathbf{A}_{/\mathbf{x}}\mathbf{x}_{/p} + \mathbf{A}_{/p} \right) \mathbf{Y} \\ &= \mathbf{A}\mathbf{Y}_{/p} + \frac{\mathrm{d}\mathbf{A}}{\mathrm{d}p}\mathbf{Y}, \end{aligned} \tag{22}$$

i.e. a problem with the same matrix $\mathbf{A}$ of the original one, forced by a term $(\mathrm{d}\mathbf{A}/\mathrm{d}p)\mathbf{Y}$ that depends on the reference solution, as also noted in Ref. [13] in the context of parameter sensitivity of nonlinear periodic problems. The term $\mathbf{A}_{/\mathbf{x}}$ is the second-order derivative of function $\mathbf{f}$ with respect to the state $\mathbf{x}$. It vanishes for linear problems. The sensitivity of the state to the parameter p is obtained by perturbing the problem $\dot{\mathbf{x}} = \mathbf{f}(\mathbf{x}, t)$,

$$\dot{\mathbf{x}}_{/p} = \mathbf{f}_{/x}\mathbf{x}_{/p} + \mathbf{f}_{/p}, \tag{23}$$

and integrating it in time accordingly. A similar problem needs to be solved for each parameter.

The sensitivity of the state transition matrix, $\mathbf{Y}_{/p}(t, t_j)$, can be calculated using an approach similar to the one that was used to calculate the state transition matrix. The derivative of Eq. (6) yields

$$\mathbf{Y}_{/p}(t, t_j) \approx \left(\mathrm{e}^{\hat{\mathbf{A}}(t-t_j)} \right)_{/p} \mathbf{Y}(t_j) + \mathrm{e}^{\hat{\mathbf{A}}(t-t_j)} \mathbf{Y}_{/p}(t_j, 0), \tag{24}$$

where the state transition matrix $\mathbf{Y}(t_j)$ and its sensitivity $\mathbf{Y}_{/p}(t_j, 0)$ are known, since they are integrated starting from $t = 0$ with $\mathbf{Y}(0) = \mathbf{I}$ and $\mathbf{Y}_{/p}(0) = \mathbf{0}$. The derivative of the matrix exponential function can be calculated using the matrix power series formula of Eq. (7),

$$\begin{aligned} \left(\mathrm{e}^{\hat{\mathbf{A}}(t-t_j)} \right)_{/p} &= \mathbf{A}_{/p}t + \frac{1}{2}(\mathbf{A}_{/p}\mathbf{A} + \mathbf{A}\mathbf{A}_{/p})t^2 \\ &+ \frac{1}{6}(\mathbf{A}_{/p}\mathbf{A}^2 + \mathbf{A}\mathbf{A}_{/p}\mathbf{A} + \mathbf{A}^2\mathbf{A}_{/p})t^3 + \ldots \\ &= \sum_{k=0}^{+\infty} \frac{1}{k!} \sum_{i=0}^{k} \mathbf{A}^i \mathbf{A}_{/p} \mathbf{A}^{k-i} t^{k+1}, \end{aligned} \tag{25}$$

which again can be approximated by truncation, e.g. for $k_{\max} = 1$, considering a small enough time step. Alternatively, more accurate estimates of the sensitivity of the state transition matrix can be computed by solving the related differential equation.

3 Example Problem Set-up

This section describes how the proposed methodology is applied to the practical case of damper design. Two aerospace problems are selected. The first one is the helicopter ground resonance, which requires dampers between the rotor hub and the blades to contrast blade motion that would displace the rotor center of mass, preventing divergent oscillations of the airframe. The second one is shimmy vibration of landing gears, which is cured by adding dampers to contrast the yaw oscillations of the tire. For both problems, a viscous damper is considered, whose damping coefficients are related to the nonlinear fluid flow. The optimization method is based on continuation, which uses the LCE estimates and their sensitivity to find the desired performance and mass values for the dampers.

3.1 Baseline Linear Models

3.1.1 Ground Resonance Model

A common, yet dangerous dynamic problem of helicopters is Ground Resonance (GR). It is a mechanical instability associated with the degrees of freedom that describe the lead-lag motion of the rotor blades [17] when the helicopter is in contact with the ground. The combination of the in-plane motion of the blades causes an overall in-plane motion of the rotor center of mass, which couples with the fixed frame pitch and roll dynamics of the airframe and undercarriage system. For this reason, the damping of the in-plane motion of the blades can be critical in articulated and soft-inplane rotor designs. In those cases, damping is usually provided by lead-lag dampers. Since these dampers are added to each blade, the cost, weight and maintenance penalty is multiplied by the number of blades, therefore a trade-off is sought between the stability margin and the mass and complexity of the damper.

Owing to its simplicity, Hammond's model [18] has been extensively used to study GR. A sketch of the model is presented in Fig. 1; the corresponding numerical values are listed in Table 1. Hammond's ground resonance model is a linear differential equation:

$$\mathbf{M}\ddot{\mathbf{x}} + \mathbf{C}\dot{\mathbf{x}} + \mathbf{K}\mathbf{x} = \mathbf{0} \tag{26}$$

which can be written in state space form as

$$\begin{Bmatrix} \dot{\mathbf{x}} \\ \ddot{\mathbf{x}} \end{Bmatrix} = \begin{bmatrix} \mathbf{0} & \mathbf{I} \\ -\mathbf{M}^{-1}\mathbf{K} & \mathbf{M}^{-1}\mathbf{C} \end{bmatrix} \begin{Bmatrix} \mathbf{x} \\ \dot{\mathbf{x}} \end{Bmatrix} \tag{27}$$

where the degrees of freedom vector is

$$\mathbf{x} = \left\{ \zeta_1 \; \zeta_2 \; \zeta_3 \; \zeta_4 \; X_h \; Y_h \right\}^T \tag{28}$$

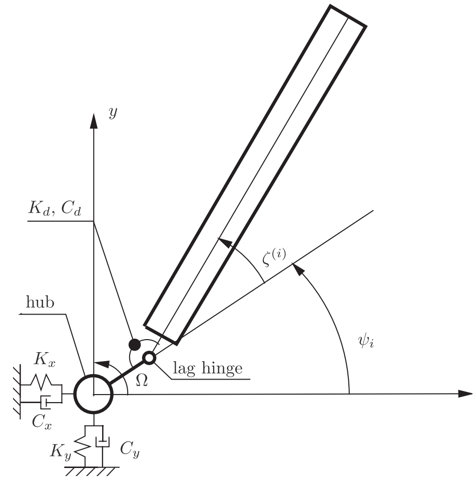

(a) Hammond's Model

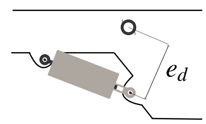

(b) Offset from lag hinge

Fig. 1: Sketch of Hammond's helicopter ground resonance model with one blade is presented for clarity (a) and typical collocation of lag damper (b).

for $\zeta_i, i = 1:4$ is the blade lead lag angle; X_h and Y_h are hub motion. The matrices of Eq. 28 are given as:

$$\mathbf{M} = \begin{bmatrix} J_\zeta & 0 & 0 & 0 & 0 & 0 \\ 0 & J_\zeta & 0 & 0 & 0 & 0 \\ 0 & 0 & J_\zeta & 0 & 0 & 0 \\ 0 & 0 & 0 & J_\zeta & 0 & 0 \\ 0 & 0 & 0 & 0 & M_x & 0 \\ 0 & 0 & 0 & 0 & 0 & M_y \end{bmatrix} + S_\zeta \begin{bmatrix} 0 & 0 & 0 & 0 & -s & c \\ 0 & 0 & 0 & 0 & -c & -s \\ 0 & 0 & 0 & 0 & s & -c \\ 0 & 0 & 0 & 0 & c & s \\ -s & -c & s & c & 0 & 0 \\ c & -s & -c & s & 0 & 0 \end{bmatrix} \tag{29a}$$

$$\mathbf{C} = \begin{bmatrix} C_\zeta & 0 & 0 & 0 & 0 & 0 \\ 0 & C_\zeta & 0 & 0 & 0 & 0 \\ 0 & 0 & C_\zeta & 0 & 0 & 0 \\ 0 & 0 & 0 & C_\zeta & 0 & 0 \\ 0 & 0 & 0 & 0 & C_x & 0 \\ 0 & 0 & 0 & 0 & 0 & C_y \end{bmatrix} + 2\Omega S_\zeta \begin{bmatrix} 0 & 0 & 0 & 0 & 0 & 0 \\ 0 & 0 & 0 & 0 & 0 & 0 \\ 0 & 0 & 0 & 0 & 0 & 0 \\ 0 & 0 & 0 & 0 & 0 & 0 \\ s & c & -s & -c & 0 & 0 \\ -c & s & c & -s & 0 & 0 \end{bmatrix} \tag{29b}$$

$$\mathbf{K} = \begin{bmatrix} K_\zeta & 0 & 0 & 0 & 0 & 0 \\ 0 & K_\zeta & 0 & 0 & 0 & 0 \\ 0 & 0 & K_\zeta & 0 & 0 & 0 \\ 0 & 0 & 0 & K_\zeta & 0 & 0 \\ 0 & 0 & 0 & 0 & K_x & 0 \\ 0 & 0 & 0 & 0 & 0 & K_y \end{bmatrix} + \Omega^2 S_\zeta \begin{bmatrix} e & 0 & 0 & 0 & 0 & 0 \\ 0 & e & 0 & 0 & 0 & 0 \\ 0 & 0 & e & 0 & 0 & 0 \\ 0 & 0 & 0 & e & 0 & 0 \\ s & -c & s & c & 0 & 0 \\ -c & s & c & -s & 0 & 0 \end{bmatrix} \tag{29c}$$

where $s = \sin\psi$, $c = \cos\psi$, being $\psi = \Omega t$ the azimuth angle of the first blade. Note that although the equations are time dependent, they can be written in time invariant form using multiblade coordinates [19]. However, since Lyapunov Exponents are estimated as the system evolves in time, using multiblade coordinates is not necessary. The nonlinear terms can be added to the linear state space form as a forcing function:

$$\begin{Bmatrix} \dot{\mathbf{x}} \\ \ddot{\mathbf{x}} \end{Bmatrix} = \begin{bmatrix} \mathbf{0} & \mathbf{I} \\ -\mathbf{M}^{-1}\mathbf{K} & -\mathbf{M}^{-1}\mathbf{C} \end{bmatrix} \begin{Bmatrix} \mathbf{x} \\ \dot{\mathbf{x}} \end{Bmatrix} + \begin{Bmatrix} \mathbf{0} \\ \mathbf{M}^{-1}\mathbf{f}_{NL} \end{Bmatrix} \quad (30)$$

Table 1: Numerical values of Hammond ground resonance model parameters [18].

Number of blades	N	4	
Blade static moment	S_ζ	189.1	kg m
Blade inertia	J_ζ	1084.7	kg m^2
Lag hinge offset	e	0.3	m
Lag spring	K_ζ	0.0	N m rad^{-1}
Lag damper	C_ζ	4067.5	N m rad^{-1}s
Hub mass	M_x	8026.6	kg
	M_y	3283.6	kg
Hub damper	C_x	51.0	kN s m^{-1}
	C_y	25.5	kN s m^{-1}
Hub spring	K_x	1240.4	kN m^{-1}
	K_y	1240.4	kN m^{-1}

3.1.2 Shimmy Vibration of Landing Gears

Shimmy is a self-excited oscillation of an aircraft landing gear as a result of dynamic forces between the tires and the ground during high-speed taxiing, e.g. during take-off and landing [20]. Mounting a damper with an offset from the steering axis is a typical solution to dissipate the oscillation energy [21]. The damper is designed according to the desired stability characteristics of the overall landing gear system. There are several methods for the stability analysis of shimmy vibration, one of them being the usual eigenanalysis after linearization [22]. Although eigenvalues are effective and provide quantitative stability indications, this type of analysis is limited to linear models. Considering that the shimmy dampers used in various aircraft have nonlinear damping characteristics [23], LCEs can be used to generalize the stability analysis of shimmy vibrations to non-linear, time dependent models. Moreover, LCE sensitivity to design parameters can help optimizing the design of the damper. To illustrate this claim, a simplified yaw dynamics of a landing gear is adopted from [24]. As presented in Fig. 2, the model includes the yaw (ψ) and lateral motion of the leading point of tire ground contact (y). The equations of motion for the linear yaw dynamics with nonlinear damper are expressed in the form $\dot{\mathbf{x}} = \mathbf{A}\mathbf{x}$ with:

$$\mathbf{A} = \begin{bmatrix} 0 & 1 & 0 \\ -\frac{k_\psi}{I_z} & -\frac{c_\psi}{I_z} - \frac{\kappa}{V I_z} & \frac{F_z\left(C_{M\alpha} - e_c C_{F\alpha}\right)}{I_z\sigma} \\ V & e_c - a & \frac{V}{\sigma} \end{bmatrix}, \mathbf{x} = \begin{Bmatrix} \psi \\ \dot{\psi} \\ y \end{Bmatrix} \quad (31)$$

where the variables are defined and reported in Table 2. The nonlinear terms can be added to the linear state space form as a forcing function:

$$\dot{\mathbf{x}} = \mathbf{A}\mathbf{x} + \mathbf{f}_{NL} \quad (32)$$

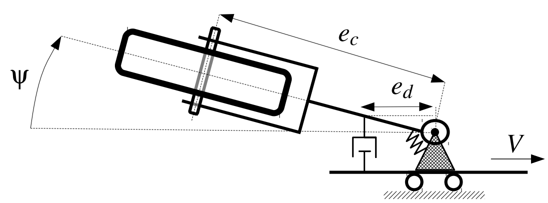

Fig. 2: Idealized yaw motion dynamics of a landing gear

3.2 Nonlinear Damper

Hammond's ground resonance and shimmy vibration models are linear. Both result from the linearization of several contributions, ranging from geometrical to constitutive. In this work, they are referred to as baseline, and modified with non-linear blade lead-lag dampers. In this work, the design optimization is performed on a viscous damper, which is very popular and finds several applications, ranging from automotive suspensions [25] to helicopter rotor blades [26]. The constitutive nonlinearity of hydraulic lead-lag dampers is considered, using a typical viscous damper as presented in Fig. 3. The damping force is assumed to be sum of a linear and a quadratic term:

$$F_d = C_L\dot{x} + C_Q|\dot{x}|\dot{x} \quad (33)$$

Table 2: Numerical values of shimmy vibration model [24].

Forward Velocity	V	$50\ \mathrm{m\,s^{-1}}$
Caster length	e_c	0.12 m
Damper distance	e_d	0.30 m
Yaw damping	c_ψ	Variable $\mathrm{N\,m\,s\,rad^{-1}}$
Yaw stiffness	k_ψ	$380000\ \mathrm{N\,m\,rad^{-1}}$
Half contact length	a	0.1 m
Relaxation length	$\sigma = 3a$	0.3 m
Vertical force	F_z	150 kN
Moment derivative	$C_{M\alpha}$	$-1\ \mathrm{m\,rad^{-1}}$
Side force derivative	$C_{F\alpha}$	$0.002\ \mathrm{rad^{-1}}$
Tire damping	κ	$570\ \mathrm{N\,m^2\,rad^{-1}}$
Inertia	I_z	$100\ \mathrm{kg\,m^2}$

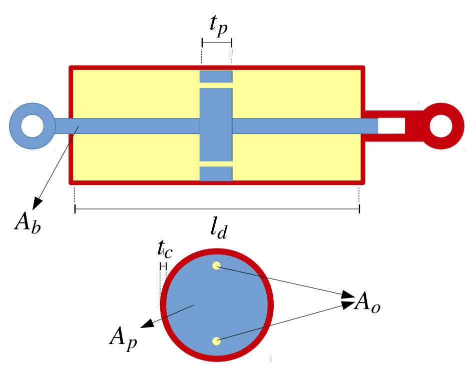

(a) Damper Parameters

Fig. 3: Cross section of a typical viscous damper

which is added to the baseline models as a forcing contribution.

In order to link the damping terms to some design parameters, linear and quadratic damping coefficients as functions of the geometric parameters are used, according to [27]:

$$C_L = \frac{8\mu l \pi r_p^4}{r_o^4} \qquad C_Q = \frac{3\rho\pi r_p^6}{4 r_o^4} \tag{34}$$

To contribute to the dynamics equations, the translational damper must be converted to a rotational one by connecting it to hub and blade with an offset e_d, such that, neglecting geometric nonlinear terms, $x \approx e_d\zeta$; thus $\delta\zeta \cdot M_d = \delta x \cdot F_d$, which yields $M_d = e_d F_d = e_d^2 C_L \dot{\zeta} + e_d^3 C_Q |\dot{\zeta}|\dot{\zeta}$; then:

$$C_\zeta = e_d^2 C_L \qquad C_{\zeta^2} = e_d^3 C_Q \tag{35}$$

The linear damping term is already included in the state space form as described above. The nonlinear term is added as a forcing function to the baseline models. The forcing function for the ground resonance problem is:

$$\mathbf{f}_{NL} = -C_{\zeta^2}\left\{|\dot{\zeta}_1|\dot{\zeta}_1 \ |\dot{\zeta}_2|\dot{\zeta}_2 \ |\dot{\zeta}_3|\dot{\zeta}_3 \ |\dot{\zeta}_4|\dot{\zeta}_4 \ 0 \ 0\right\}^T \tag{36}$$

similarly, the forcing function for the shimmy vibration problem is given as:

$$\mathbf{f}_{NL} = -C_{\zeta^2}/I_z\left\{0 \ |\dot{\psi}|\dot{\psi} \ 0\right\}^T \tag{37}$$

In addition to the linear and nonlinear damping coefficients, which are important in stability evaluation, the mass of the dampers is also important, since it introduces a weight penalty. Therefore, the mass should be considered in a design optimization by either not allowing it to increase while achieving better stability properties, or minimizing it while preserving a satisfactory level of energy dissipation. As such, the mass and the stability measure are chosen as the two critical objectives and/or constraints of the viscous damper design. The sketch in Fig. 3 is used for the preliminary estimation of the mass of the damper,

$$\begin{aligned} m &= m_f + m_p + m_c \\ &\approx \rho_f\left[(A_p - A_b)(l_d - t_p) + A_o t_p\right] \\ &+ \rho_p\left[(l_d - t_p)A_b + t_p(A_p - A_o)\right] \\ &+ \rho_c\left[2 r_p t_c l_d + 2 A_p t_c\right], \end{aligned} \tag{38}$$

where the radius of the piston is $r_p = \sqrt{A_p/\pi}$. The assumed numerical values are reported in Table 3.

It is worth noticing that the method can be applied to more complex damper types and constitutive relationships; their formulation can be included in the LCE estimation as long as the details explained in Section 2 are followed.

3.3 Optimization Formulation

The analytical sensitivity of the stability indicators can be used with any gradient-based or gradient-aware optimization technique. In order to demonstrate the use

Table 3: Assumed geometry and properties of damper

Piston Area	A_p	variable	mm^2
Orifice Area	A_o	variable	mm^2
Piston Thickness	t_p	30	mm
Cylinder thickness	t_c	5	mm
Damper Length	l_d	19.2	mm
Fluid Density*	ρ_f	850	kg m^{-3}
Kinematic viscosity*	ν	25	mm^2 s^{-1}
Metal Density	ρ_m	7800	kg m^{-3}
Damper offset	e_d	300	mm

* typical aviation hydraulic fluid values at 20^o

of the proposed method, a continuation approach is considered [28, 29]. This approach has been selected to better keep under control the number of iterations performed in the analysis, since LCE estimation and the evaluation of their sensitivity can be very computationally expensive. Continuation starts from an initial configuration and tracks the stability indicators in the presence of equality constraints [30]. It can be occasionally implemented as an optimization tool [31] and can be used in design and bifurcation analysis (see for example [28, 32, 33]).

Suppose that a set of critical stability indicators are being tracked, which are parametrized by a set of independent parameters $\mathbf{p} = [\Delta p_1, \ldots, \Delta p_n]$:

$$\lambda_i(\Delta p_1, \ldots, \Delta p_n) = 0 \tag{39}$$

where i goes from 1 to the number of stability indicators N_λ. Furthermore, differentiable functions of the parameters can be added, which constrain the parameter changes:

$$g_j(\Delta p_1, \ldots, \Delta p_n) = 0 \tag{40}$$

where j goes from 1 to the number of constraints N_g. The stability indicators and constraint functions are differentiated with respect to each parameter to solve for the required amount of parameter change $\Delta\mathbf{p}$ in the neighborhood of the parameters $\mathbf{p}$ at the current iteration. In matrix form,

$$\begin{bmatrix} \lambda_{1/p_1} & \cdots & \lambda_{1/p_n} \\ \vdots & \vdots & \vdots \\ \lambda_{N_\lambda/p_1} & \cdots & \lambda_{N_\lambda/p_n} \\ g_{1/p_1} & \cdots & g_{1/p_n} \\ \vdots & \vdots & \vdots \\ g_{N_g/p_1} & \cdots & g_{N_g/p_n} \end{bmatrix} \begin{Bmatrix} \Delta p_1 \\ \vdots \\ \Delta p_{N_p} \end{Bmatrix} = \begin{Bmatrix} \Delta b_1(\mathbf{p}) \\ \vdots \\ \Delta b_{N_\lambda+N_g}(\mathbf{p}) \end{Bmatrix} \tag{41}$$

or, in compact form,

$$\mathbf{S}\Delta\mathbf{p} = \mathbf{b} \tag{42}$$

The constraint sensitivities and right-hand side vector only include terms that are already known or calculated. Then, the required amount of parameter change in the parameter vector $\Delta\mathbf{p}$ is

$$\Delta\mathbf{p}_n = \mathbf{S}_n^{-1}\mathbf{b}_n \tag{43}$$

which is defined when the number of variables is equal to the number of equations, $N_p = N_\lambda + N_g$. In case of an underdetermined system, when $N_p > N_\lambda + N_g$, a minimum norm solution is obtained using the Moore-Penrose pseudo-inverse, or the problem can be made strictly determined using additional constraints. If the problem is overdetermined, i.e. $N_p < N_\lambda + N_g$, the problem can only be solved in a least squares sense, which however may imply a violation of the constraints. The minimum norm solution can be influenced by appropriately weighting the equations.

As long as the amount of change $\Delta\mathbf{p}_n$ is computed, the parameters are iteratively updated as

$$\mathbf{p}_{n+1} = \mathbf{p}_n + \alpha\Delta\mathbf{p}_n, \tag{44}$$

where an optional multiplier α ($0 < \alpha \leq 1$) can be used to limit the parameter increment and achieve smoother convergence. The continuation procedure starts from an initial set of parameters. At each step n, the sensitivity of the LCEs ($\lambda_{/p}$) is estimated using the method described in Section 2. Iterations continue until convergence is achieved, for $\Delta\mathbf{p}$ that converges to zero.

In this work we aim at minimizing the mass of the damper with an inequality constraint on the largest LCE, $\lambda_{\max} \leq \lambda_{\text{des}} = -0.5$ rad s^{-1}. Not exceeding a specified value for the largest LCE is intended as a safe requirement in terms of stability (e.g. to achieve a desired amplitude halving time). Although more sophisticated stability performances can be defined, the present one is considered appropriate to illustrate the use of the proposed formulation for LCE sensitivity evaluation.

The strategy is to choose between two constraint vectors:

$$\Delta \mathbf{p} = \begin{cases} \mathbf{S}^{-1}\mathbf{b}_{CM} & \lambda > \lambda_{\text{des}} \\ \mathbf{S}^{-1}\mathbf{b}_{MM} & \lambda \leq \lambda_{\text{des}} \end{cases} \tag{45}$$

which force the parameters to keep the mass constant and achieve the limiting LCE if the largest allowed LCE constraint is violated; otherwise, the continuation is performed to achieve both minimum mass and desired LCE. Therefore, the open form of the sensitivity matrix and right hand side vectors are:

$$\mathbf{S} = \begin{bmatrix} \lambda_{/A_p} & \lambda_{/A_o} \\ m_{/A_p} & m_{/A_o} \end{bmatrix} \tag{46}$$

$$\mathbf{b}_{CM} = \begin{Bmatrix} \lambda_{\text{des}} - \lambda(A_p, A_o) \\ 0 \end{Bmatrix} \tag{47}$$

$$\mathbf{b}_{MM} = \begin{Bmatrix} \lambda_{\text{des}} - \lambda(A_p, A_o) \\ m_{\min} - m(A_p, A_o) \end{Bmatrix} \tag{48}$$

where $m_{\min}$ is the minimum allowable damper mass, prescribed to be 3.0 kg based on the structural mass represented by metal parts and a limit amount of liquid to make the damper operate as required.

Using the described strategy and limits for the mass and largest LCE, the damper mass is minimized using three different initial values for the largest LCE, $\lambda_{\text{max,iv}}$: 1) $\lambda_{\text{max,iv}} > \lambda_{\text{des}}$, 2) $\lambda_{\text{max,iv}} = \lambda_{\text{des}}$, and 3) $\lambda_{\text{max,iv}} < \lambda_{\text{des}}$. The initial area setting that yields $\lambda_{\text{max,iv}} = \lambda_{\text{des}}$ case is referred to as "nominal", and is used to normalize the results. The initial mass is set to the same value for the three cases. For each case, the optimization using continuation is summarized in a top-down fashion as follows:

1) start from an initial set of design parameters: $\mathbf{p}_0 = [A_o \;\; A_p]^T$;
2) estimate sensitivity of LCEs ($\lambda_{/A_o}, \lambda_{/A_p}$) and damper mass ($m_{/A_o}, m_{/A_p}$) to each design parameter;
3) form the sensitivity matrix (Eq. 46) and constraint matrices (Eqs. 47 and 48);
4) solve for the required amount of parameter change $\Delta\mathbf{p}$ based on the prescribed LCE constraint (Eq. 45);
5) calculate the new set of nominal values of the parameters $\mathbf{p}_{n+1}$ (Eq. 44);
6) if $|\mathbf{p}_{n+1} - \mathbf{p}_n| < \varepsilon$ for a small enough ε, terminate; otherwise repeat steps 2 to 5 until convergence is achieved.

4 Results and Discussion

This section presents the results of design optimization of nonlinear dampers to achieve a desired performance for the problems described in Section 3, using the analytical sensitivity computed as described in Section 2. The validation of the analytical sensitivity of LCEs is presented first. Then, the results are presented for the two demonstration cases, which aim at minimization of damper mass while guaranteeing an acceptable level of damper performance.

4.1 Validation

The analytical sensitivity of LCEs was verified in a previous work, [14], using several models, including a variant of the current one. The LCEs estimated as functions of the linear damping coefficient C_L are first shown in Fig. 4(a). Then, for the same range of linear damping coefficient, the analytical LCE sensitivity estimation is compared in Fig. 4(b) with the values obtained applying finite differences to those of Fig. 4(a). The plots of Figure 4 show the two largest LCEs of the problem. For values of the linear damper coefficient from 0 to about 30 % of the nominal value, the largest one is about zero, indicating that the fiducial trajectory is a limit cycle. For values greater than 30 % of the nominal value, the two LCEs take the same value (i.e. the corresponding LCE has multiplicity equal to 2), and decrease along a nearly straight line. The sensitivity values obtained with the proposed procedure are in reasonably good agreement with the corresponding valued obtained through finite differences.

4.2 Case I: Ground Resonance

For the ground resonance problem, we aim at minimizing the mass of the damper with an inequality constraint on the largest LCE, $\lambda_{\text{des}} \leq -0.5\ \text{rad s}^{-1}$. The minimum allowable damper mass is prescribed to be $m_{\min} = 3.0$ kg based on the structural mass induced by metal parts and a limit amount of liquid to make the damper operate as required.

Using the described strategy and limits for the mass and largest LCE, the damper mass is minimized using three different initial values for the largest LCE, $\lambda_{\text{max,iv}}$: 1) $\lambda_{\text{max,iv}} > -0.5\ \text{rad s}^{-1}$, 2) $\lambda_{\text{max,iv}} = -0.5\ \text{rad s}^{-1}$, and 3) $\lambda_{\text{max,iv}} < -0.5\ \text{rad s}^{-1}$. The initial area setting that yields $\lambda_{\text{max,iv}} = -0.5\ \text{rad s}^{-1}$ case is referred to as "nominal", and is used to normalize the results. The initial damper mass is set to $m_0 = 10.0$ kg for all three cases.

Fig. 5 presents the continuation of these three cases. It can be observed that all three cases converge to the same area settings, largest LCE at $\lambda_{max} = -0.5\ \text{rad s}^{-1}$, and minimum mass of approximately 3 kg. The two cases which start from equal or smaller maximum LCE

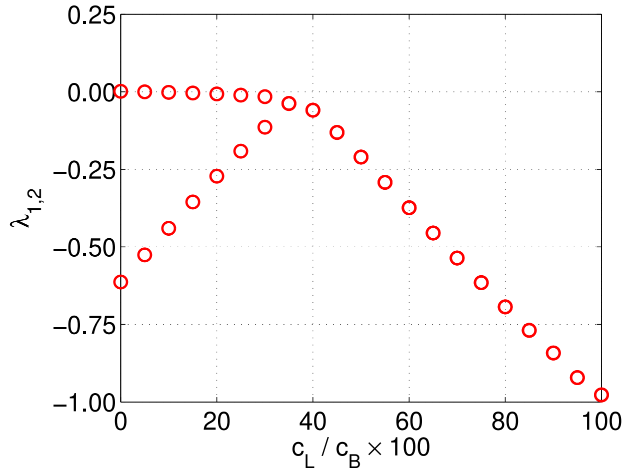

(a) 2 largest LCEs

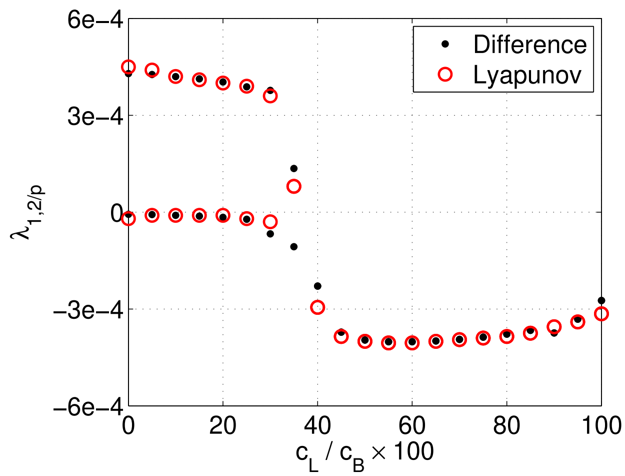

(b) Sensitivity of 2 largest LCEs

Fig. 4: The analytical sensitivity of LCEs to linear damping coefficient is compared and validated using discrete derivative of previously calculated LCEs

converge with a similar smooth trend; convergence is achieved within 5 iterations. On the contrary, the case with an initial value of λ greater than the limit value behaves differently, since in that case the largest LCE first aims at satisfying the constraint while keeping the initial mass constant, and then converges to the same results of the other two cases within about 10 iterations. During this process, almost 100% of the computer resources are spent on the estimation of LCE and its sensitivity. Although the code is not optimized for speed, 700 s average wall clock time is observed for one iteration.

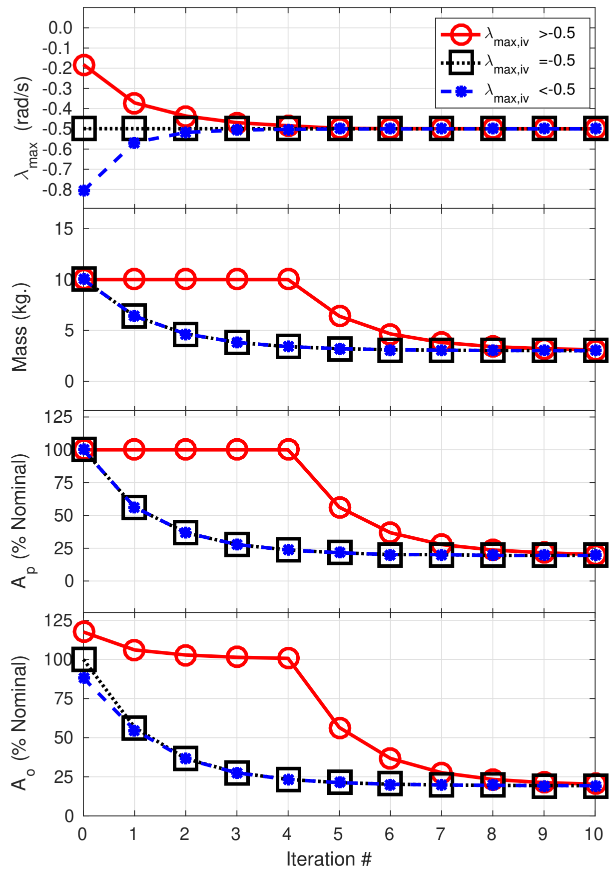

Fig. 5: Ground resonance: Design of blade damper for a minimum mass while ensuring the value of largest LCE estimate at a given value. Initial and desired values are: $m_0 = 10$ kg, $m_{\min} = 3$ kg, $\lambda_{\max} = -0.5$ rad s^{-1}.

4.3 Case II: Shimmy Vibration

Similar to the ground resonance problem, we aim at minimizing the mass of the damper attached to a landing gear to damp shimmy vibrations. The chosen inequality constraint on the largest LCE value is $\lambda_{\max} \leq \lambda_{\text{des}} = -1.0$ rad s^{-1}. The minimum allowable damper mass is set again to $m_{\min} = 3.0$ kg. Using the previously described strategy and limits for the mass and largest LCE, the damper mass is minimized using three different initial values for the largest LCE, $\lambda_{\max,\text{iv}}$: 1) $\lambda_{\max,\text{iv}} > -1.0$ rad s^{-1}, 2) $\lambda_{\max,\text{iv}} = -1.0$ rad s^{-1}, and 3) $\lambda_{\max,\text{iv}} < -1.0$ rad s^{-1}. The initial area setting that yields $\lambda_{\max,\text{iv}} = -1.0$ rad s^{-1} case is referred to as "nominal", and is used to normalize the results. The initial mass of the damper is set to $m_0 = 6.0$ kg for all three cases.

Fig. 6 presents the continuation of the three cases for the shimmy vibration problem. It can be observed that all three cases converge to the same area settings, largest LCE at $\lambda_{max} = -1.0$ rad s^{-1}, and minimum mass of approximately 3 kg. The two cases which start from maximum LCE equal to or smaller than the desired value converge with a smooth trend similar to the results of Fig. 5. During this process, almost 100% of the computer resources are spent on the estimation of LCE and its sensitivity. Although the code is not optimized for speed, 200 s average wall clock time is observed for one iteration.

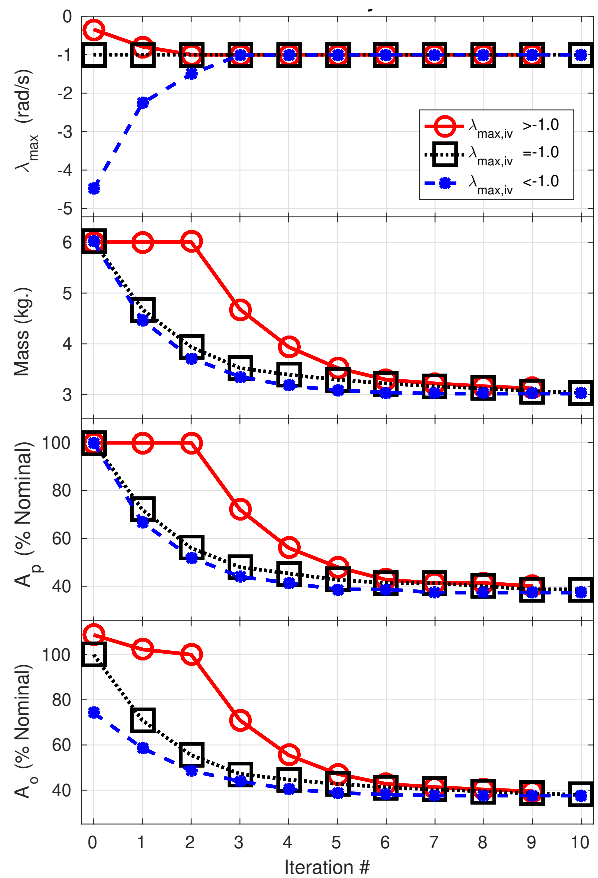

Fig. 6: Shimmy Vibration: Design of a shimmy damper for minimum mass while ensuring the value of the largest LCE estimate at a given value. Initial and desired values are: $m_0 = 6$ kg, $m_{min} = 3$ kg, $\lambda_{max} = -1.0$ rad s^{-1}.

5 Conclusions

The use of the analytical sensitivity of Lyapunov Characteristic Exponents in design optimization of nonlinear dynamical systems is presented. The LCE estimation and its analytical sensitivity formulation is based on the discrete QR method. Both the LCE and their sensitivity are evaluated while the nonlinear problem evolves. This eliminates the necessity of calculating LCE values with different parameter values to estimate their sensitivity by finite differences, therefore achieving more accurate sensitivity estimations within a shorter time and reduced or comparable computational cost. The design optimization is demonstrated using a continuation technique, although it is worth stressing that any gradient-based algorithm can benefit from the proposed formulation. Ground Resonance of helicopters and shimmy vibration of landing gears are selected as the reference numerical examples, using well known linear models modified by adding nonlinear viscous blade dampers. The tracking of parameters with mass and stability constraints are presented. It is shown that the analytical sensitivity of LCEs makes it possible to consider the nonlinearities and time-dependencies during design optimization without simplifying the problem as linear, time-invariant.

References

[1] Hirsch, M. W., Smale, S., and Devaney, R. L., 2004. *Differential Equations, Dynamical Systems, and an Introduction to Chaos*. Elsevier, San Diego, California.

[2] Medio, A., and Lines, M., 2001. *Nonlinear Dynamics — A Primer*. Cambridge University Press.

[3] Strogatz, S. H., 1994. *Nonlinear Dynamics and Chaos: With Applications to Physics, Biology, Chemistry, and Engineering*. Perseus Books, Reading, Massachusetts.

[4] Adrianova, L. Y., 1995. *Introduction to Linear Systems of Differential Equations*, Vol. 146 of *Translations of Mathematical Monographs*. American Mathematical Society, Providence, Rhode Island.

[5] Hodges, D., and Pierce, G. A., 2002. *Introduction to Structural Dynamics and Aeroelasticity*. Cambridge University Press, Cambridge, England.

[6] Dowell, E. H., 2015. *A Modern Course in Aeroelasticity*, 5th ed. Springer.

[7] Benettin, G., Galgani, L., Giorgilli, A., and Strelcyn, J.-M., 1980. "Lyapunov characteristic exponents for smooth dynamical systems and for Hamiltonian systems; a method for computing all of them. part 1: Theory". *Meccanica,* **15**(1), March, pp. 9–20. doi:10.1007/BF02128236.

[8] Cong, N. D., and Nam, H., 2003. "Lyapunov's inequality for linear differential algebraic equation". *Acta Mathematica Vietnamica,* **28**(1), pp. 73–88.

[9] Cong, N. D., and Nam, H., 2004. "Lyapunov regularity of linear differential algebraic equations of index 1". *Acta Mathematica Vietnamica,* **29**(1), pp. 1–21.

[10] Masarati, P., 2013. "Estimation of Lyapunov exponents from multibody dynamics in differential-algebraic form". *Proc. IMechE Part K: J. Multi-body Dynamics,* **227**(4), pp. 23–33. doi:10.1177/1464419312455754.

[11] Rao, S., 1996. *Engineering Optimization: Theory and Practice*, 3rd ed. John Wiley & Sons.

[12] Krauskopf, B., Osinga, H. M., and Galán-Vioque, J., 2007. *Numerical continuation methods for dynamical systems*. Springer.

[13] Shih, I.-C., Spence, A. M., and Celi, R., 1996. "Semianalytical sensitivity of Floquet characteristic exponents with application to rotary-wing aeroelasticity". *Journal of Aircraft,* **33**(2), pp. 322–330. doi:10.2514/3.46941.

[14] Masarati, P., and Tamer, A., 2015. "Sensitivity of trajectory stability estimated by Lyapunov characteristic exponents". *Aerospace Science and Technology,* **47**, November, pp. 501–510. doi:10.1016/j.ast.2015.10.015.

[15] Tamer, A., and Masarati, P., 2016. "Stability of nonlinear, time-dependent rotorcraft systems using Lyapunov characteristic exponents". *Journal of the American Helicopter Society,* **61**(2), pp. 1–12. doi:10.4050/JAHS.61.022003.

[16] Dieci, L., and Van Vleck, E. S., 2002. "Lyapunov spectral intervals: Theory and computation". *SIAM Journal on Numerical Analysis,* **40**(2), pp. 516–542. doi:10.1137/S0036142901392304.

[17] Coleman, R. P., and Feingold, A. M., 1958. Theory of self-excited mechanical oscillations of helicopter rotors with hinged blades. Report 1351, NACA.

[18] Hammond, C. E., 1974. "An application of Floquet theory to prediction of mechanical instability". *Journal of the American Helicopter Society,* **19**(4), pp. 14–23. doi:10.4050/JAHS.19.14.

[19] Bir, G., 2008. "Multiblade coordinate transformation and its application to wind turbine analysis". In 46th AIAA Aerospace Sciences Meeting and Exhibit. doi:10.2514/6.2008-1300.

[20] Tourajizadeh, H., and Zare, S., 2016. "Robust and optimal control of shimmy vibration in aircraft nose landing gear". *Aerospace Science and Technology,* **50**, pp. 1 – 14. doi=10.1016/j.ast.2015.12.019.

[21] Li, Y., Jiang, J. Z., and Neild, S., 2016. "Optimisation of shimmy suppression device in an aircraft main landing gear". *Journal of Physics: Conference Series,* **744**(1), p. 012066. doi:10.1088/1742-6596/744/1/012066.

[22] Somieski, G., 1997. "Shimmy analysis of a simple aircraft nose landing gear model using different mathematical methods". *Aerospace Science and Technology,* **8**, February, pp. 547–555. doi=10.1016/S1270-9638(97)90003-1.

[23] Besselink, I., 2000. "Shimmy of aircraft main landing gears". PhD thesis, TU Delft.

[24] Arreaza, C., 2015. "Linear stability analysis, dynamic response, and design of shimmy dampers for main landing gears". Master's thesis, University of Toronto, Toronto, Canada.

[25] Jugulkar, L. M., Singh, S., and Sawant, S. M., 2016. "Analysis of suspension with variable stiffness and variable damping force for automotive applications". *Advances in Mechanical Engineering,* **8**(5), p. 1687814016648638. doi=10.1177/1687814016648638.

[26] Marathe, S., Gandhi, F., and Wang, K. W., 1998. "Helicopter blade response and aeromechanical stability with a magnetorheological fluid based lag damper". *Journal of Intelligent Material Systems and Structures,* **9**(4), pp. 272–282. doi=10.1177/1045389X9800900405.

[27] Li, Z. Q., Xu, Y. L., and Zhou, L. M., 2006. "Adjustable fluid damper with sma actuators". *Smart Materials and Structures,* **15**(5), p. 1483. doi:10.1088/0964-1726/15/5/038.

[28] Tamer, A., and Masarati, P., 2013. "Linearized structural dynamics model for the sensitivity analysis of helicopter rotor blades". In Ankara International Aerospace Conference.

[29] Tamer, A., and Masarati, P., 2014. "Periodic stability and sensitivity analysis of rotating machinery". In Proceedings of the 9th International Conference on Rotor Dynamics IFToMM ICORD 2014. doi:10.1007/978-3-319-06590-8_170.

[30] Cardani, C., and Mantegazza, P., 1976. "Continuation and direct solution of the flutter equation". *Computers & Structures,* **8**(2), pp. 185–192. doi:10.1016/0045-7949(78)90021-4.

[31] Kim, I. Y., and Kwak, B. M., 2002. "Design space optimization using a numerical design continuation method". *International Journal of Numerical Methods in Engineering,* **53**, pp. 1979–2002. doi=10.1002/nme.369.

[32] Rezgui, D., Lowenberg, M. H., Jones, M., and Monteggia, C., 2014. "Continuation and bifurcation analysis in helicopter aeroelastic stability problems". *J. of Guidance, Control, and Dynamics,* **37**(3), pp. 889–897. doi:10.2514/1.60193.

[33] Jones, M., Bernascone, A., Masarati, P., Quaranta, G., and Rezgui, D., 2014. "Ongoing developments in the use of continuation-bifurcation methodology at AgustaWestland". In 40th European Rotorcraft Forum.